International Journal of Earth Sciences Knowledge and Applications
journal homepage: http://www.ijeska.com/index.php/ijeska

Research Article e-ISSN: 2687-5993

Integration of ASTER and Airborne Radiometric Data in the Exploration for Hydrothermal Alteration Zones Associated with Mineral Deposits in Igarra Schist Belt, Nigeria

Moses Uyota Ohwo[1]*, Fadeyi Simeon Solape[2]

[1]*Department of Geology, University of Benin, Benin City, Nigeria*
[2]*Nigeria Geological Survey Agency, Nigeria*

INFORMATION

Article history
Received 29 July 2024
Revised 31August 2024
Accepted 31 August 2024

Keywords
F-parameter
Band rationing
Sericite
K-deviation
Potassium alteration

Contact
*Moses Uyota Ohwo
moses.ohwo@physci.uniben.edu

ABSTRACT

Advanced Spaceborne Thermal Emission and Reflection Radiometer imagery and airborne radiometric data were integrated in order to map hydrothermal alteration zones associated Igarra Schist Belt, Nigeria. Band rationing (BR) and False colour composite (FCC) image processing techniques were performed on the ASTER imagery to map alteration minerals while, F-parameter and K-deviation methods were applied on the airborne radiometric data tin mapping diagnostic hydrothermal alteration zones associated with mineralization. The Advanced Spaceborne Thermal Emission and Reflection Radiometer imagery data mapped phyllic, argillic, propylitic, ferric oxides, ferrous oxides, and gossans alteration minerals in the VNIR and SWIR bands of the Advanced Spaceborne Thermal Emission and Reflection Radiometer system. While the F-parameter and K-deviation methods performed on the radiometric data indicated potassium (K) alteration zones varying from 0.0 – 0.4 and -1.0 – 2.3, respectively.

1. Introduction

Hydrothermal alteration has been recognized as a significant "mineralization system" in primary mineral deposits globally in various geological environments, including the study area (Di Tommaso and Rubinstein, 2007; Maden and Akaryali, 2015; Sanusi and Amigun, 2020).

Obaje (2009) recognized various hydrothermal alteration processes such as silica metasomatism, argillic alteration, and chloritic (propylitic) alteration and fluorization. The granites and meta-sedimentary rocks, which are common in the research area, have been discovered to be altered by hydrothermal processes. Mineral exploration has benefitted from the use of satellite imagery data for mapping lithological differences in rocks (Sabins, 1999) as well as for mapping different alteration zones related to mineral deposits (Gabr et al., 2021).

Through the analysis of the reflectance patterns of various wavelengths of satellite images, geologists can distinguish between the different lithologic units, and alteration zones which aids mineral exploration. Similarly, remote sensing is instrumental in mapping alteration zones, which are indicative of mineralization potential. Alteration minerals often exhibit distinctive spectral features that can be detected using specialized sensors such as Advanced Spaceborne Thermal Emission and Reflection Radiometer (ASTER); Landsat, etc., allowing for the identification of mineralized zones associated with hydrothermal alteration (Sabins, 1999; Gad and Kusky 2006; Qiu et al., 2006; Amer et al., 2010; Gabr et al., 2010; Abu El-Magd et al., 2015; Emam et al., 2016). Presently, remote sensing methods are considered a vital tool for appraising areas with mineral potential. Both satellite and airborne sensors have always provided useful information especially when integrated with other exploration techniques such as radiometric (Frassy et al., 2015). Alteration zones represent the overflow of the deep mineralized bodies and represent the zones in which the hydrothermal fluids migrated and deposited their mineralized fluids (Pour and Hashim, 2015; Zoheir et al., 2019). Hydrothermal alteration is an important index in the mineral exploration which involves the introduction of hydrothermal fluids containing chemical composition complexes depending on the rock and fluid ratio (Rushmer, 1991; Robb, 2005). It is subsequently followed by the reworking and remobilization of mineral deposits through assimilation in country rocks under favorable temperature and pressure conditions (Akinlalu, 2023). This in turn causes changes in both the chemical composition and mineralogy of rocks (Phillips and Powell, 2010; McCauig and Hronsky, 2014). This then permits the mapping of anomalous changes in rocks caused by hydrothermal alteration using geophysical methods (Sanusi and Amigun, 2020).

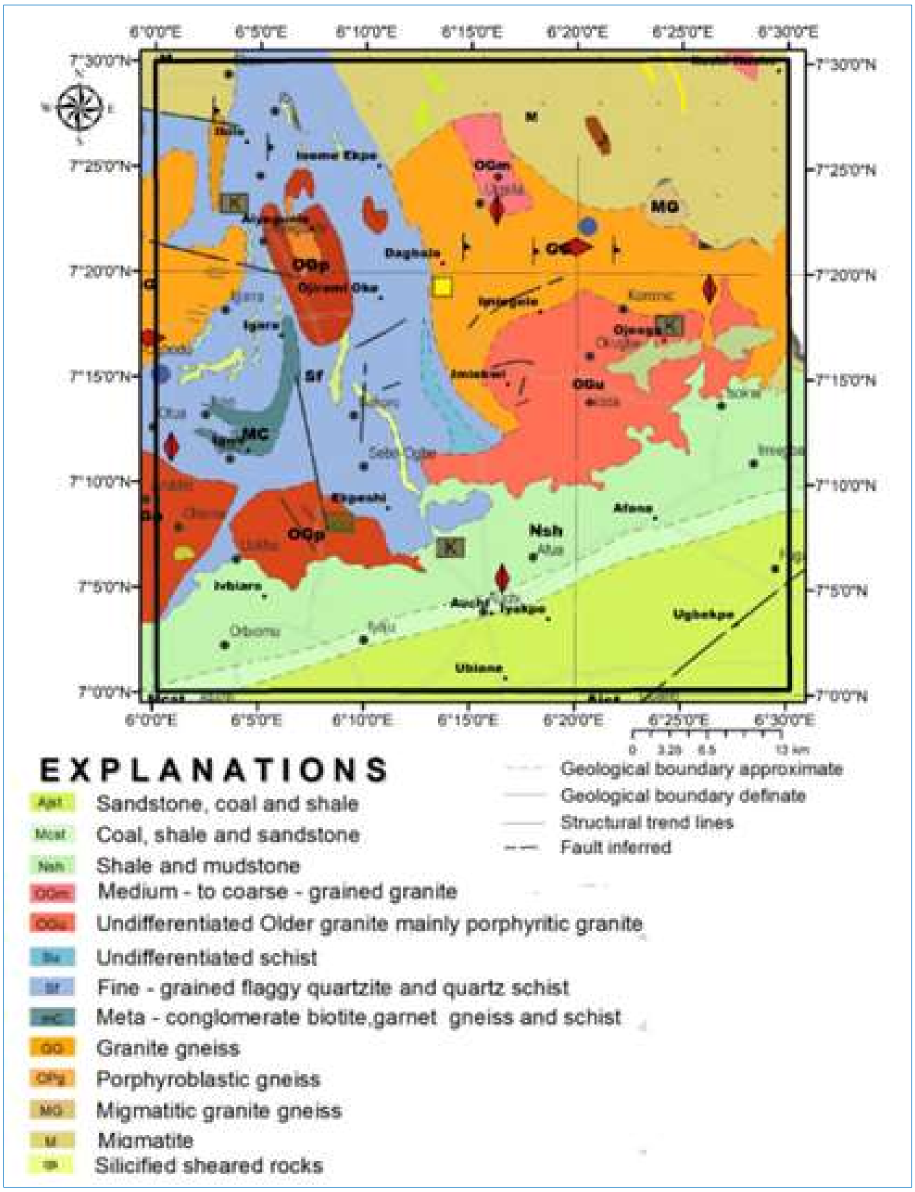

Fig. 1. Dahomey Basin is shown on a regional Gulf of Guinea map in respect to other basins (Adapted from Brownfield et al., 2006)

The mapping of hydrothermal alteration zones can thus be accomplished with the integration of both radiometric and satellite (ASTER) Imagery (Eleraki et al., 2017; Sanusi and Amigun, 2020). However, the radiometric approach offers the most detailed on the discovery and identification of alteration minerals that are indicators for mapping hydrothermal alteration zones (Maden and Akaryali, 2015; Eleraki et al., 2017). This is because direct identification of potassium enriched zones through potassic alteration, genetically linked to gold mineralization can be delineated easily through the distribution of radioelements like Potassium (K), Thorium (Th) and Uranium (U) (Graham and Bonham-Carter, 1993; Grasty and Shives, 1997; Wilford et al., 1997; Ford et al., 2000; Abd El Nabi, 2013; Eleraki et al., 2017; Sanusi and Amigun, 2020; Olomo et al., 2022).

The radioelement contents of geological units that are undergoing deformation can alter in a variety of ways due to hydrothermal processes (Eleraki et al., 2017). Radiometric methods are useful for mapping potassic alteration, which is a significant aspect of hydrothermal alteration (Akinlalu, 2023). Other important alterations like argillic, propylitic, iron oxides, gossans, and phyllic alteration that are also genetically linked to mineralization are mapped through ASTER (Andogma et al., 2020; Forson et al., 2022). Hence, the integration of ASTER satellite imagery and airborne radiometric data to enhance both the accuracy and efficiency in mapping hydrothermal alteration zones. The current study focuses on mapping promising areas of mineralization (hydrothermal alteration) zones in the ISB, Nigeria, fusing airborne radiometric data and ASTER imagery.

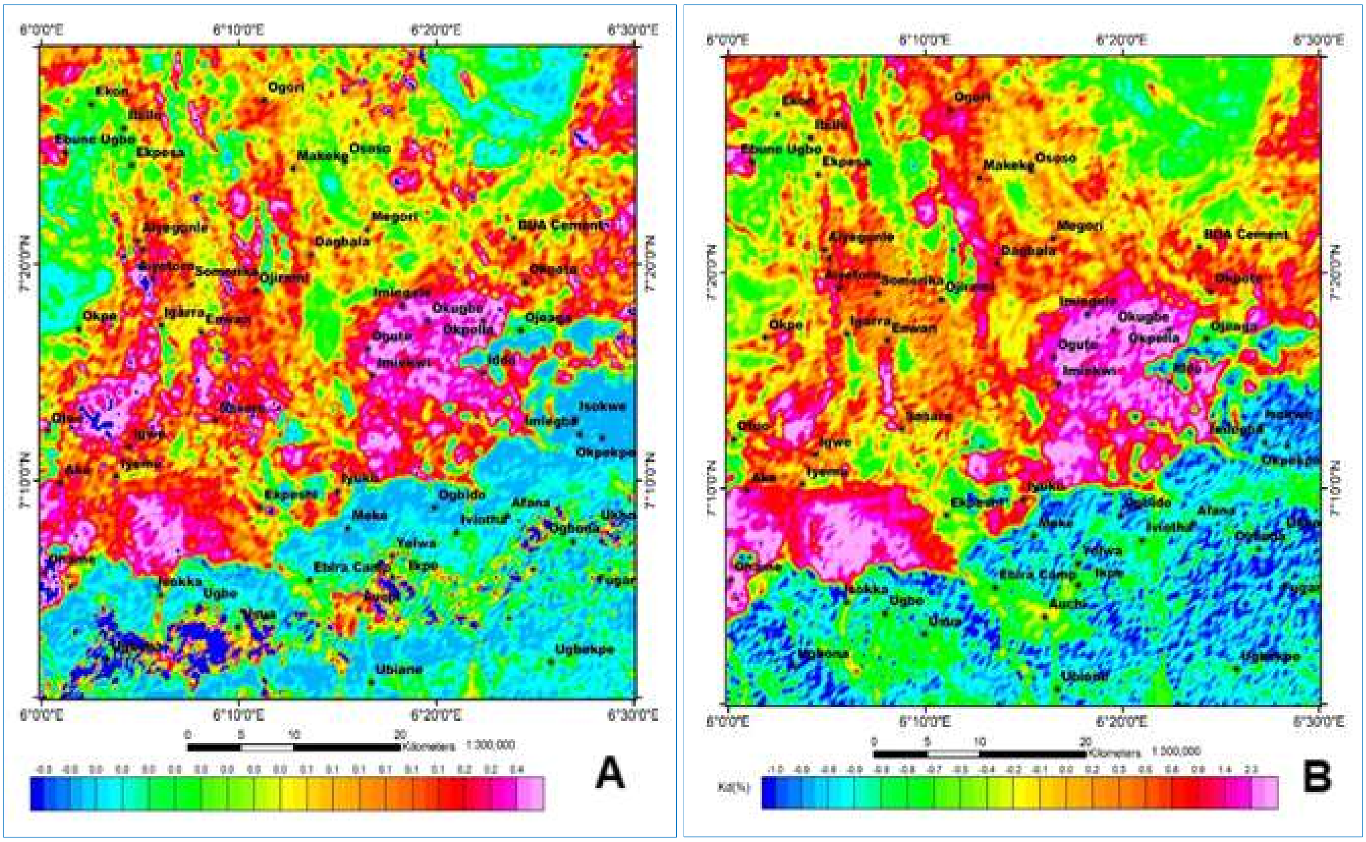

Fig. 2. (A) F-parameter and (B) K-ideal maps

2. Geologic and Tectonic Settings

The research location is situated within the Igarra Schist Belt (ISB) underlain by rock units of the migmatite-gneiss complex (MGC), Pan African Granitoids (PAG), and the low-grade metasediments (LGM), (Odeyemi, 1976; 1988), (Fig. 1). The ISB occurs as N-S trending zone of low to medium grade metasediments such as phyllite, semi-pelitic to pelitic schist, metagreywacke, meta-conglomerate, quartzite and basic to ultrabasic metavolcanics (Fig. 1), (Rahaman, 1988; McCurry, 1989; Annor, 1998).

Boesse and Ocan (1992) reported that the belt has been affected by at least two phases of orogeny (deformation): the first phase (D1) produced tight to isoclinal folds with north-southerly direction while the second phase (D2) is characterized by more open folds of variable style with large vertical NNE-SSW trending fault. Geological features such as folds and faults are common in the metasedimentary rocks and intruded by mainly quartz veins inclined in the northeast to southwest direction (Fig. 1). The rock units coupled with the quartzites appear as lenses of bands in the undifferentiated schists which dominate the region.

Most parts of the study area are underlain by the metasediments, which presumably overlies the older MGC, possibly of Liberian age (Odeyemi, 1976).

While the southern part of the study region consists of sedimentary rock units comprising sandstone, coal and shale, shale and mudstone (Fig. 1). The ISB have the prospect of hosting mineralization this is due to the fact that the schist belt is similar to the gold bearing schist belts in Northern Nigeria (Woakes et al., 1978; Adekoya, 1978; Garba, 2002).

3. Materials and Methods

3.1. Materials

The materials used in this study comprises ASTER imagery data, and airborne radiometric data. The ASTER imagery data was acquired from the United States Geological Survey (USGS) agency earth explorer website, processed and interpreted using ArcGIS 10.8 and ENVI 5.3 software programs. While the airborne radiometric data was acquired from the Nigerian Geological Survey Agency (NGSA), processed and interpreted using Geosoft Oasis Montaj software.

3.2. Methodology

3.2.1. ASTER Imagery Data

One of the ASTER level-1B ITT Visual Information Solutions' ENVI 5.3 (ENVI) image processing and analysis software and Environmental Systems Research Institute's ArcGIS 10.8 were utilized in order to process the cloud-free data that was collected on December 15, 2021. The data collected covered the whole study region. Based on the solar zenith angle, satellite view angle, and relative azimuth angle between the satellite and sun image parameters, the ASTER images were translated from a sensor radiance to the top of the atmospheric reflectance. This transformation was accomplished with the help of the calibration utilities provided by ENVI. According to Laben (2000), the Gram-Schmidt Pan-Sharpening method was utilized to combine the ASTER VNIR images, which had a pixel size of 15 meters, with the six band SWIR image, which had a pixel size of 30 meters, in order to improve the spatial features. A nine-band ASTER image with a resolution size of 15 meters was produced by stacking the fused SWIR image with the VNIR image. This image includes both the VNIR and SWIR bands from the original image. Contemporary studies of Pour and Hashim (2015), Rajendran et al. (2013), Di Tommaso and Rubinstein (2007) and Salem et al. (2013) utilized the VNIR-SWIR spectral bands of ASTER with image processing techniques such as band ratios (BR) and False Colour Composite (FCC) in delineating lithology, hydrothermally altered zones, and mineralized zones.

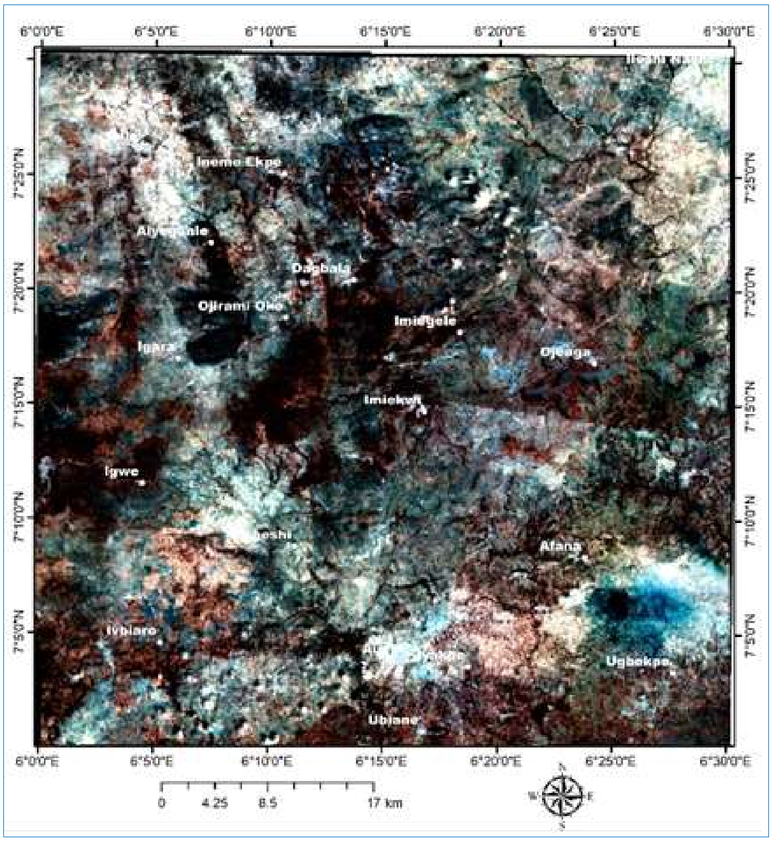

Fig. 3. VNIR-SWIR FCC image indicating argillic-phyllic and propylitic alterations in red-pink (amethystine) and green tones

3.2.2. Airborne Radiometric Data

The radiometric survey that was carried out by Fugro Airborne survey between 2002 and 2009 with 512-channel gamma-ray spectrometers (with crystals measuring 2 inches by 2 inches). The single-band percentage potassium (% K), equivalent thorium and uranium (eTh and eU) pseudo colour images derived from the radiometric data were used to map lithology (Wilford, 1997).

The single-band % K, eTh, and eU pseudo colour images were used for interpretation because they indicate areas where a particular radio-element can be directly correlated with the geochemical properties of the surface lithology and regolith (Chisambi et al., 2021). In order to map and differentiate potassic alteration zones induced by hydrothermal alteration from areas of K-enrichment caused by other processes such as weathering and leaching (Abd El-Nabi, 2013; Akinlalu, 2023), the mathematical expression (equation 1) known as the F-parameter, established by Efimov (1978), was employed for this task (*Equation 1*).

$$F = K^{*}eU/eTh = K/eTh/eU = eU/eTh/K \qquad (1)$$

The F-parameter, which was created by Efimov (1978), is an important marker of hydrothermal alteration in rocks (Maden and Akaryali, 2015). This is because it is a reflection of the ratio of eTh to eU as well as the concentration of %K. According to Eleraki et al. (2017), locations with a high anomaly factor are considered to have been hydrothermally altered. Additionally, the potassium deviation (Kd), mathematical expression (*Equation 2*) introduced by Saunders et al. (1987), has been proven to be appropriate and diagnostic in identifying hydrothermal alteration zones linked with mineralization (Akinlalu, 2023) was also used in mapping hydrothermal alteration zones.

$$K_n = (K_{avg} / Th_{avg}) * Th \quad (2)$$

4. Results and Discussion

4.1. Airborne Radiometric Data

4.1.2. Potassium Alteration Anomaly (Kd) and F-Parameter Maps

In order to map hydrothermally altered zones associated with K-enrichment diagnostically, mathematical combinations: Kd and F-parameter proposed by Saunders et al. (1987) and Efimov (1978) respectively were combined to produce abundance ratios which are diagnostic of alterations in rocks (Erdi-Krausz et al., 2003; De Quadros et al., 2003; Eleraki et al., 2017). The Kd map (Fig. 2A) depicts diverge distribution of K that isolates hydrothermally altered areas with anomalously high Kd values regarded as hydrothermally altered areas (Eleraki et al., 2017). The Kd map is a true method for identifying hydrothermally altered areas since it is able to delineate areas that are likely to have been affected by hydrothermal processes. The Kd map illustrated in Fig. 2A, has anomaly values that range from -1.0 to 2.3%. The hydrothermally altered regions are identified by the presence of high Kd anomalies, which manifest themselves as large irregular concentric halos at the central, southwestern, and elongated strips and patches on the northern flanks. The anomaly values in these regions range from 0.9 to 2.3%.

Additionally, anomaly values ranging from 0.0 to 0.4 is indicated on the F-parameter map (Fig. 2B). In addition to isolated patches of occurrences in the map's edges, these anomalous zones can be found on the middle and western flanks of the map (Fig. 2B). Also, the presence of porphyritic granite, granite gneiss, and migmatite gneiss coincides with the presence of these anomalously high areas. Anomaly expressions are also observed on the schistose rocks due to their close proximity to the granitoids. Generally, it is observed that potassic alteration and sericitization which are important in mineralization, has major occurrence on the granitoids, thereby making areas proximal to them to be hydrothermally altered (Grasty and Shives, 1997).

4.2. ASTER Imagery Data

4.2.1. FCC

FCC was applied to identify alteration minerals. The creation of false color composite is based on known spectral properties of rocks and alteration minerals in relation to the selected spectral bands (Fakhari et al., 2019). Rocks that have undergone argillic and phyllic alteration as well as propylitic and carbonate alteration may be distinguished using different colors of ASTER bands 468 in RGB (red, green and blue) (Ali-mohammadi et al., 2015; Di Tommaso and Rubinstein, 2007). Examination of the FCC image (Fig. 3) depicts argillic and phyllic altered rocks (muscovite and sericite) in reddish to pink (amethystine) tones, propylitic alteration (chlorite and epidote) in green tones as a result of the absorption of Al-OH (centred at ASTER band 6) and Fe-, Mg-O-H (at ASTER band 8) absorption features respectively.

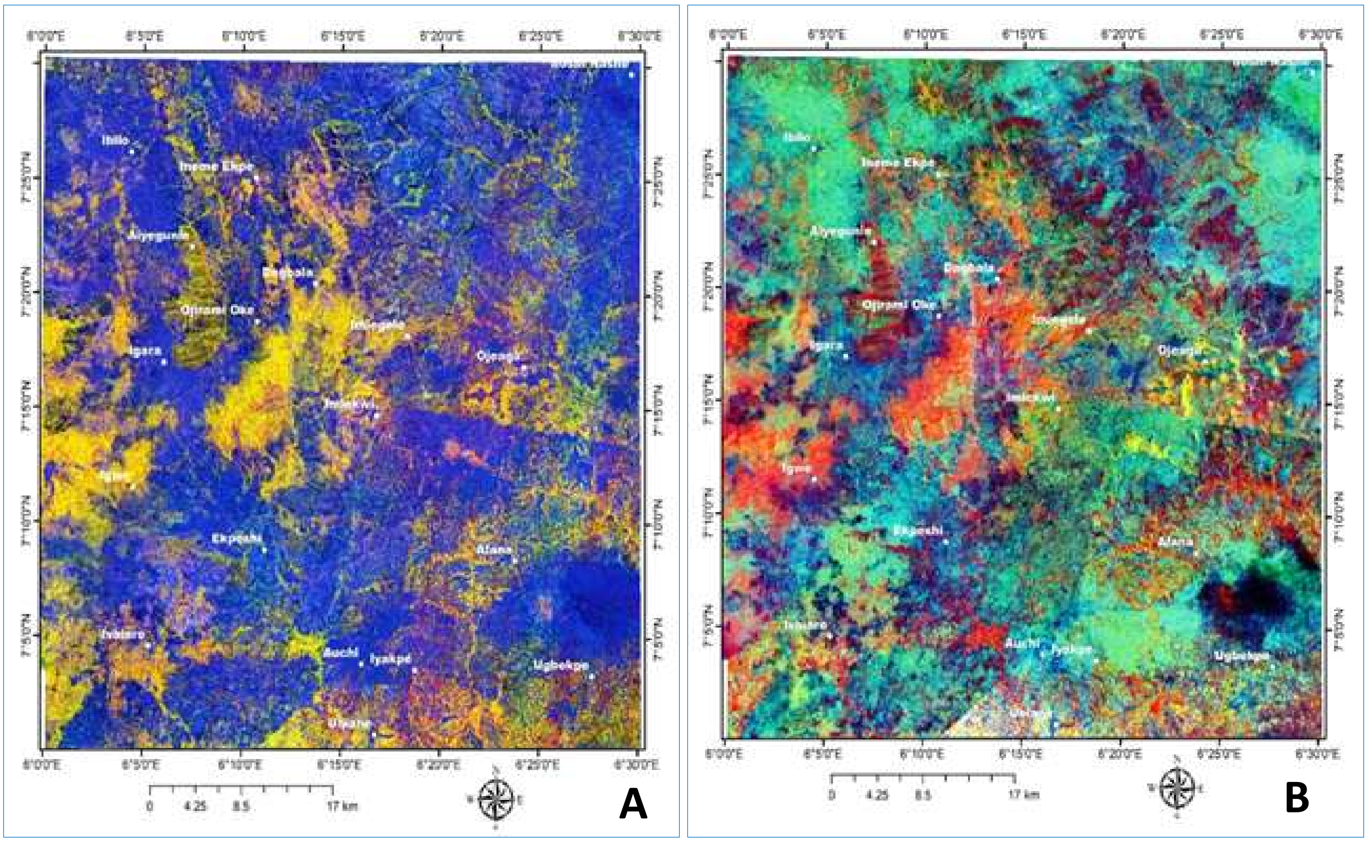

Fig. 4. (A) ASTER VNIR-SWIR BR of phyllic, argillic, propylitic, and iron oxides alterations; and (B) Iron oxides in red, non-mineralized rocks in green, mineralized rocks in pink/purple colours

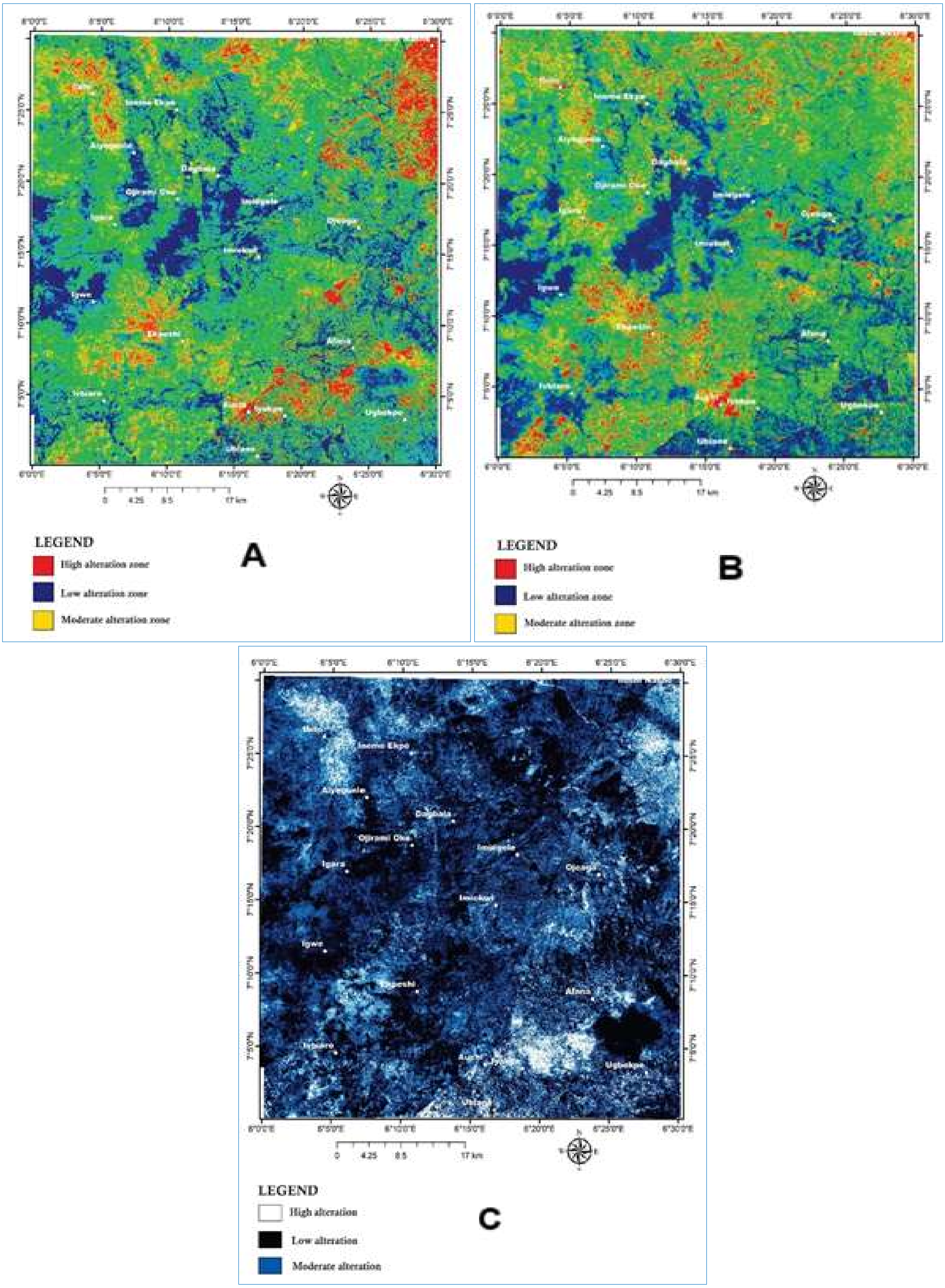

Fig. 5. (A): VNIR-SWIR band ratio image of ferric iron, (B): ferrous iron and (C) gossan alterations

4.2.2. Band Rationing (BR)

In lithologic and alteration mapping, the band ratio (BR) method is frequently used to improve the spectral differences between bands that can be built based on the spectral features of the rocks and minerals (Jiang et al., 2014; Nair and Mathew, 2012; Rowan et al., 2006). The band ratio combinations of 4/6, 5/8, and 2/1 were selected on the basis of the reflectance spectra obtained from JPL (Fig. 4A) in order to enhance, respectively, the phyllic-and-argillic-altered rocks (muscovite and kaolinite with Al-OH absorption), the propylitic-altered rocks (chlorite, epidote, and carbonates), and the iron oxides. The examination of Fig. 4A reveals that rocks with phyllic and argillic changed properties (muscovite and kaolinite with Al-OH absorption) are colored in red tones by using B4/B6, rocks with propylitic altered properties (chlorite, epidote, and carbonates) are colored in yellow tones by using B5/B8, and iron oxides are colored in blue tones by using B2/B1.

Better separation of the mineralized portions of the alteration zones was achieved using the following ASTER bands; (4/8, 4/2, and 8/9 in RGB respectively) (Fig. 4B). To improve the reaction of the iron oxides (Fig. 4B) in the changed mineralized rocks, the BR 4/8 was adopted and to further distinguish the altered mineralized rocks from both altered non-mineralized and unaltered rocks, BR 4/2 was adopted while, BR 8/9 was used for improved contrast. Further examination of Figure 4B depicts BR 4/8 (iron oxides) in red, BR 4/2 (altered non-mineralized and the unaltered rocks) in green, and BR 8/9 (improved contrast) in blue, mineralized parts of the alteration zones in pink and purple tones.

4.2.3. Simple Band Ratio

Depending on the spectral properties of alteration minerals, a change in the abundance of an alteration mineral in an altered rock would result in a modest change in the reflectance value for both altered and unaltered rocks, Sabins (1997). Altered rocks exhibit increased red reflectance in the visible spectrum due to the iron enrichment of the rock, whereas the unaltered rocks show lower reflectance in band 7 than band 5. Figure 5 (A, B and C) depicts regions of mineralized altered rocks with high iron oxide (ferric and ferrous iron) content using the rationing of B2/B1 and B5/B3 + B1/B2 proposed by (Rowan et al., 2013) which is suitable for the mapping of iron oxides alteration which have the potential to host mineral deposits, and in the identification of alteration minerals and regolith occurring as gossans. Band ratio (B4/B2) for the mapping of gossans modified after Volesky et al., (2003) was used. Gossans can be utilized as hints to the presence of underground ore deposits since they are created by the oxidation of the sulphide minerals in an ore deposit, especially if characteristic box works are present. Fig. 5A-C, depicts ferric iron and ferrous iron alterations in red, yellow and blue coloration as high, moderate and low alterations respectively. While gossans alteration (Fig. 5C) is depicted in white, dark-blue and black coloration as high, moderate and low alterations respectively.

5. Conclusion

The airborne gamma ray spectrometric delineated hydrothermal alteration zones of the study region. The results airborne gamma ray spectrometric data indicated hydrothermally altered areas that are associated with the granites and schistose rock units in the study region. While the ASTER data in the VNIR and SWIR bands mapped phyllic, argillic, propylitic, iron oxides and gossans alteration zones in the study region.

6. Recommendation

Rock geochemical survey analysis should be conducted to confirm the alteration minerals revealed in the alteration zones indicated by the ASTER imagery and airborne radiometric data.

Declaration of competing interest

We declare that we do not have any commercial or associative interest that represents a conflict of interest in connection with the work.

Acknowledgement

The author appreciates the efforts of G.O. Ohwo and A.A. Adepelumi for their immense contribution to the success of this research.

References

Abd El Nabi, S.H., 2013. Role of γ-ray spectrometry in detecting potassic alteration associated with Um Ba'anib granitic gneiss and metasediments, G. Meatiq area, Central Eastern Desert, Egypt. Arabian Journal of Geosciences 6, 1249-1261. https://doi.org/10.1007/s12517-011-0378-4.

Abu El-Magd, I., Mohy, H., Basta, F., 2015. Application of remote sensing for gold exploration in the Fawakheir area, Central Eastern Desert of Egypt. Arabian Journal of Geosciences 8, 3523-3536.

Adekoya, J.A., 1978. Gold Deposits in Nigeria: A Summary of Available Information. Kaduna South: Special Report of Geological Survey of Nigeria.

Akinlalu, A.A., 2023. Radiometric Mapping for The Identification of Hydrothermally Altered Zones Related to Gold Mineralization in Ife–Ilesa Schist Belt, Southwestern Nigeria. Indonesian Journal of Earth Sciences 3 (1), A519. https://doi.org/10.52562/injoes.2023.519.

Ali-Mohammadi, M., Alirezaei, S., Kontak, D.J., 2015. Application of ASTER data for exploration of porphyry copper deposits, a case study of Daraloo–Sarmeshk area, southern part of the Kerman copper belt, Iran. Ore Geology Reviews 70, 290-304.

Amer, R., Kusky, T., Ghulam, A., 2010. Lithological mapping in the Central Eastern Desert of Egypt using ASTER data. Journal of African Earth Science 56, 75-82.

Andongma, W.T., Gajere, J.N., Amuda, A.K., Edmond, R.R.D., Faisal, M., Yusuf, Y.D., 2021. Mapping of hydrothermal alterations related to gold mineralization within parts of the Malumfashi Schist Belt, North Western Nigeria. The Egyptian Journal of Remote Sensing and Space Science 24 (3), 401-417. https://doi.org/10.1016/j.ejrs.2020.11.001.

Annor, A.E., 1998. Structural and chronological relationship between the low grade Igarra schist and adjoining Okene Migmatite-Gneiss terrain in the Precambrian exposure of Southwestern Nigeria. Journal. Mining and Geology 34, 197-194.

Boesse, S., Ocan, O., 1992. Geology and evolution of the Ife-Ilesha Schist belt, southwestern Nigeria, In Benin-Nigeria Geotraverse, International Meeting on the Proterozoic Geology and Tectonics of High-Grade Terrain, IGCP 215, 123-129.

Chisambi, J., Haundi, T., and Tsokonombwe, G., 2021. Geologic structures associated with gold mineralization in the Kirk Range area in Southern Malawi. De Gruyter. Open Geosciences 13, 1345-1357. https://doi.org/10.1515/geo-2020-0304.

De Quadros, T.F.M., Koppe, J.C., Strieder, J.C., Costa, J.F.C.L., 2003. Gamma-Ray Data Processing and Integration for Lode-Au Exploration. Natural Resources Research 12, 57-65. http://dx.doi.org/10.1023/A:1022608505873.

Di Tommaso, I., Rubinstein, N., 2007. Hydrothermal alteration mapping using ASTER data in the Infiernillo porphyry deposit, Argentina. Ore Geology Reviews 32 (1-2), 275-290. https://doi.org/10.1016/j.oregeorev.2006.05.004.

Di Tommaso, I., Rubinstein, N., 2007. Hydrothermal alteration mapping using ASTER data in the infernally porphyry deposit, Argentina. Ore Geology Reviews 32, 275-290. https://doi.org/10.1016/j.oregeorev.2006.05.004.

Efimov, A.V., 1978. Multiplikativnyj pokazatel dlja vydelenija endogennych rud poaerogamma-spektrometriceskim dannym. Metody rudnoj geofiziki. Leningrad, Naucno-Proizvodstvennoje Objedinenie Geofizika 163, 59-68.

Eleraki, M., Ghieth, B., Abd-El Rahman, N., Zamzam, S., 2017. Hydrothermal zones detection using airborne magnetic and gamma ray spectrometric data of mafic/ultramafic rocks at Gabal El-Rubshi area, Central Eastern Desert (CED), Egypt. Advances in Natural and Applied Sciences 11 (9), 182-196.

Emam, A., Zoheir, B., Johnson, P., 2016. ASTER-based mapping of ophiolitic rocks: examples from the Allaqi-Heiani suture, SE Egypt. International Geology Review 58, 525-539. https://doi.org/10.1080/00206814.2015.1094382.

Erdi-Krausz, G., Matolin, M., Minty, B., Nicolet, J.P., Reford, W. S., Schetselaar, E.M., 2003. Guidelines for radioelement mapping using gamma ray spectrometry data: also, as open access e-book. International Atomic Energy Agency (IAEA).

Fakhari, S., Jafarirad, A., Afzal, P., Lotfi, M., 2019. Delineation of hydrothermal alteration zones for porphyry systems utilizing ASTER data in Jebal-Barez area, SE Iran. Iranian Journal of Earth Sciences 11, 80-92.

Ford, K.L., Savard, M., Dessau, J.C., Pellerin, E., Charbonneau, B.W., Shives, B.K. 2001. The role of gamma-ray spectrometry in radon risk evaluation: a case history from Oka, Quebec-Geoscience-Canada-Retrieved. journals.lib.unb.ca/index.php/GC/article/view/4074.

Forson, E.D., Wemegah, D.D., Hagan, G.B., Appiah, D., Addo–Wuver, F., Adjovu, I., Otchere, F.O., Mateso, S., Menyeh, A., Amponsah, T., 2022. Data–driven multi–index overlay gold prospectivity mapping using geophysical and remote sensing datasets. Journal of African Earth Sciences 190, 104504. https://doi.org/10.1016/j.jafrearsci.2022.104504.

Frassy, F., Maianti, P., Marchesi, A., Nodari, F,R., Via, G.D., Paulis, R.D., Biffi, P.G., Gianinetto, M., 2015. Satellite remote sensing for hydrocarbon exploration in new venture areas laboratory of remote sensing (L@ RS), Politecnico di Milano - Department of Architecture, Built Environment and Construction Engineering (ABC), Via Ponzio 31, 20133 Milano, pp. 2884-2887.

Gabr, S.S., Hassan, S.M., Sadek, M.F., 2021. Application of remote sensing in detecting mineralized zones in the pan-african belt of Egypt. In: Hamimi Z, Arai S, Fowler AR, El-Bialy MZ (eds) The Geology of the Egyptian Nubian Shield. pp. 645-664. https://doi.org/10.1007/978-3-030-49771-2_23.

Gad, S., Kusky, T.M., 2006. Lithological mapping in the Eastern Desert of Egypt, the Barramiya area, using landsat thematic mapper (TM). Journal of African Earth Sciences 44, 196-202.

Garba, I., 2002. Late Pan African Tectonics and Origin of Gold Mineralization and Rare Metal Pegmatites in the Kushaka Schist Belt, Northwestern Nigeria. Journal of Mining and Geology 38, 1-12. https://doi.org/10.4314/jmg.v38i1.18768.

Graham, D.F., Bonham-Carter, G.F., 1993. Airborne radiometric data - A tool for reconnaissance geological mapping using a GIS. Photogrammetric Engineering and Remote Sensing 59 (8), 1243-1249.

Grasty, R.L., Shives, R.B.K., 1997. Applications of gamma ray spectrometry to mineral exploration and geological mapping. In Workshop presented at Exploration (Vol. 97).

Jiang, D., Liu, L., Zhou, J., Zhuang, D., 2014. Lithological discrimination of the mafic-ultramafic complex, Huitongshan, Beishan, China: Using ASTER data. Journal of Earth Science 25 (3), 529-536. https://doi.org/10.1007/s12583-014-0437-3.

Laben, C.A., 2000. Process for Enhancing the Spatial Resolution of Multispectral Imagery Using Pan-Sharpening. US Patent 6, 011, 875.

Maden, N., Akaryalı, E., 2015. Gamma ray spectrometry for recognition of hydrothermal alteration zones related to a low sulfidation epithermal gold mineralization (eastern Pontides, NE Türkiye). Journal of Applied Geophysics 122, 74-85. https://doi.org/10.1016/j.jappgeo.2015.09.003.

McCuaig, T.C., Hronsky, J.M.A., 2014. The Mineral System Concept the Key to Exploration Targeting. In K.D. Kelley & H.C. Golden, Building Exploration Capability for the 21st Century. Society of Economic Geologists. https://doi.org/10.5382/SP.18.08.

McCurry, P., 1989. A general review of the geology of the Precambrian to Lower Paleozoic rocks of Northern Nigeria. In: Kogbe, C.A. (Ed.), Geology of Nigeria, Rock View, Jos, 13-37.

Nair, A.S., Mathew, J., 2012. Application of ASTER data in geological mapping and mineral exploration. International Journal of Remote Sensing 33 (12), 3763-3780. https://doi.org/10.1080/01431161.2011.636081.

Obaje, N.G., 2009. Geology and mineral resources of Nigeria. Springer, London, Dordrecht.

Odeyemi, I.B., 1976. Preliminary Report on the Field Relationships between the Basement Complex Rocks in Igarra, Midwestern Nigeria. In: Kogbe CA, editor. Geology of Nigeria. Lagos, Nigeria: Elizabethan Publication and Co.; 1976. p. 59-63.

Odeyemi, I.B., 1988. Lithostratigraphy and structural relationships of the upper Precambrian metasediments Igarra area, Southwestern Nigeria. In: Oluyide P.O., Mbonu W.C., Ogezi A.E., Egbiniwe I.G., Ajibade A.C., Umeji A.C. (Eds.), Precambrian Geology of Nigeria. Geol Surv Nigeria: 111-125.

Olomo, K.O., Bayode, S., Alagbe, O.A., Olayanju, G.M., Olaleye, O.K., 2022. Aeromagnetic Mapping and Radioelement Influence on Mineralogical Composition of Mesothermal Gold Deposit in Part of Ilesha Schist Belt, Southwestern Nigeria. NRIAG Journal of Astronomy and Geophysics 11 (1), 177-192. https://doi.org/10.1080/20909977.2022.2057147.

Phillips, G.N., Powell, R., 2010. Formation of gold deposits: a metamorphic devolatilization model. Journal of Metamorphic Geology 28 (6), 689-718. https://doi.org/10.1111/j.1525-1314.2010.00887.x.

Pour, A.B., Hashim, M., 2015. The application of ASTER remote sensing data to porphyry copper and epithermal gold deposits. Ore Geology Reviews 44, 1-9.

Qiu, F., Abdelsalam, M., Thakkar, P., 2006. Spectral analysis of ASTER data covering part of the Neoproterozoic Allaqi-Heiani suture, southern Egypt. Journal of African Earth Sciences 44, 169-180.

Rahaman, M.A., 1988. Recent advances in the study of the basement complex of Nigeria. In: Geological Survey of Nigeria (Ed.) Precambrian Geol Nigeria, pp 11-43.

Rajendran, S., Nasir, S., Kusky, T.M., Ghulam, A., Gabr, S., El Ghali, M., 2013. Detection of hydrothermal mineralized zones associated with Listwaenites rocks in the Central Oman using ASTER data. Ore Geology Reviews 53, 470-488.

Robb, L., 2005. Introduction to ore-forming processes. Blackwell Science Ltd, London, pp 166-173.

Rowan, L.C., Hook, S.J., Abrams, M.J., Mars, J.C., 2013. Mapping hydrothermally altered rocks at Cuprite, Nevada, using the advanced spaceborne thermal emission and reflection radiometer (ASTER), a new satellite-imaging system. Economic Geology, 98 (5), 1019-1027. https://doi.org/10.2113/gsecongeo.98.5.1019.

Rowan, L.C., Schmidt, R.G., Mars, J.C., 2006. Distribution of hydrothermally altered rocks in the Reko Diq, Pakistan mineralizedarea based on spectral analysis of ASTER data. Remote Sensing of Environment 104, 74-87.

Rushmer, T., 1991. Partial melting of two amphibolites: contrasting experimental results under fluid-absent conditions. Contributions to Mineralogy and Petrology 107 (1), 41-59. https://doi.org/10.1007/BF00311184.

Sabins, F.F., 1999. Remote sensing for mineral exploration. Ore Geology Reviews 14, 157-183.

Salem, S.M., Soliman, N.M., Ramadan, T.M., Greiling, R.O., 2013. Exploration of new gold occurrences in the alteration zones at the Barramiya District, Central Eastern desert of Egypt using ASTER data and geological studies. Arabian Journal of Geosciences 7, 1717-1731.

Sanusi, S.O., Amigun, J.O., 2020. Structural and hydrothermal alteration mapping related to orogenic gold mineralization in part of Kushaka schist belt, North-central Nigeria, using airborne magnetic and gamma-ray spectrometry data. SN Applied Sciences 2, 1-26. https://doi.org/10.1007/s42452-020-03435-1.

Saunders, D.F., Terry, S.A., Thompson, C.K., 1987. Test of national uranium resource evaluation gamma-ray spectral data in petroleum reconnaissance. Geophysics 52 (11), 1547-1556. https://doi.org/10.1190/1.1442271.

Volesky, J.C., Stern, R.J., Johnson, P.R., 2003. Geological control of massive sulfide mineralization in the Neoproterozoic Wadi Bidah shear zone, southwestern Saudi Arabia, inferences from orbital remote sensing and field studies. Precambrian Research 123 (2-4), 235-247. https://doi.org/10.1016/S0301-9268(03)00070-6.

Wilford, J.R., Bierwirth, P.E., Craig, M.A., 1997. Application of airborne gamma-ray spectrometry in soil/regolith mapping and applied geomorphology. AGSO Journal of Australian Geology and Geophysics 17 (2), 201-216.

Wilford, J., 1997. Airborne gamma ray spectrometry: Cooperative research centre for landscape environments and mineral exploration. Geosci Aust., 46-52.

Woakes, M., Rahaman, M.A., Ajibade, A.C., 1987. Some Metallogenetic Features of the Nigerian Basement. Journal of African Earth Sciences 6, 54-64.

Zoheir, B., Emam, A., Harraz, H.Z., 2019. Hydrothermal alteration and gold mineralization in the Um Rus area, Central Eastern Desert, Egypt: Implications for exploration. Ore Geology Reviews 107, 1-19. https://doi.org/10.1016/j.oregeorev.2019.02.001.